Nanoscale

PAPER

View Article Online
View Journal | View Issue

Cite this: *Nanoscale*, 2016, **8**, 12599

Mucin-mediated nanocarrier disassembly for triggered uptake of oligonucleotides as a delivery strategy for the potential treatment of mucosal tumours†

A. Martirosyan,[a] M. J. Olesen,[a] R. A. Fenton,[b] J. Kjems[a] and K. A. Howard*[a]

Received 16th October 2015,
Accepted 11th December 2015

DOI: 10.1039/c5nr07206a

www.rsc.org/nanoscale

This work demonstrates gastric mucin-triggered nanocarrier disassembly for release of antisense oligonucleotides and consequent unassisted cellular entry as a novel oral delivery strategy. A fluorescence activation-based reporter system was used to investigate the interaction and mucin-mediated disassembly of chitosan-based nanocarriers containing a 13-mer DNA oligonucleotide with a flanked locked RNA nucleic acid gapmer design. Gastric mucins were shown to trigger gapmer release from nanocarriers that was dependent on the interaction time, mucin concentration and N : P ratio with a maximal release at N : P 10. In contrast to siRNA, naked gapmers exhibited uptake into mucus producing HT-MTX mono-cultures and HT-MTX co-cultured with the carcinoma epithelial cell line Caco-2. Importantly, *in vivo* gapmer uptake was observed in epithelial tissue 30 min post-injection in murine intestinal loops. The findings present a mucosal design-based system tailored for local delivery of oligonucleotides that may maximize the effectiveness of gene silencing therapeutics within tumours at mucosal sites.

Introduction

Epithelial carcinomas account for 80–90% of all cancer cases[1] with colorectal cancer estimated to be the second cause of cancer death in the EU.[2] For the year 2015 the mortality rates per 100 000 from colorectal cancer is 16.6 in men and 9.4 in women, representing 13% of total cancer deaths. These alarming epidemiological data indicate that there is a need to explore new therapeutics.

RNA interference (RNAi)-mediated interruption of protein expression by a wide repertoire of RNAi trigger molecules offers immense potential for cancer treatment by silencing genes involved in tumour development and progression.[3–5] Successful therapeutic applications of RNAi, however, are dependent on efficient delivery to the cancer tissue and cells in order to facilitate knockdown of targeted transcripts. The mucosal surface lining the gastrointestinal (GI) tract is an attractive alternative to intravenous administration by which to target intestinal diseases.[6–8] The oral route offers ease of administration and patient compliance, with a possibility to treat both local and systemic conditions. Delivery systems, however, are required to overcome gastric degradation and the combined barrier of closely packed epithelial cells and an overlying mucus gel.[9] Mucus is a viscoelastic protective gel composed predominately of mucins that form a heterogeneous network of polymeric fibers with pores of ~200–300 nm in diameter.[10,11]

Numerous nanoparticle-based solutions have been developed to overcome the mucosal delivery barriers to RNAi-based therapeutics.[4,7,12] The utilisation of mucoadhesive materials such as the polysaccharide chitosan that interact with mucus can reduce mucosal clearance and improves the bioavailability of drugs.[13,14] Chitosan has been successfully used by our group to form polyelectrolyte nanocarrier assemblies (polyplexes) with small interfering RNA (siRNA) that exhibit gene silencing effects at pulmonary epithelial sites.[15–17] Furthermore, gastrointestinal protection, deposition and translocation into peripheral tissue of intact siRNA were demonstrated after the oral gavage of chitosan/siRNA nanocarriers in mice.[18] Microscopic detection showed a continuous fluorescent layer at the intestinal apical surface and an absence of punctuate fluorescence associated with intact particles, within the epithelial cells or submucosa; suggesting a degree of decomplexation of the nanocarriers at the mucus/epithelial interface.[18] Further work by our group revealed mucin-triggered disassembly of chitosan/siRNA nanocarriers and concomitant diffusion of free siRNA on contact with porcine gastric mucins using an *in vitro* gastric mucin microfluidic model system.[19] The

[a]*Interdisciplinary Nanoscience Center (iNANO), Department of Molecular Biology and Genetics, Aarhus University, Aarhus C, Denmark. E-mail: kenh@inano.au.dk*
[b]*Department of Biomedicine, Aarhus University, Aarhus C, Denmark*
†Electronic supplementary information (ESI) available. See DOI: 10.1039/c5nr07206a

inability of naked siRNA, however, to penetrate cellular membranes as a consequence of macromolecular and polyanionic properties suggests a necessity to incorporate nucleic acids capable of cellular entry following nanocarrier disassembly. It has been shown that short antisense oligonucleotides can enter the cells unassisted in the absence of transfection agents by a process of gymnosis and mediate gene silencing.[20,21] Furthermore, antisense oligonucleotide designs composed of locked nucleic acid (LNA) single-stranded RNA/DNA oligonucleotides, termed gapmers, exhibit increased biological stability and gene silencing activity.[20,22] Antisense oligonucleotide-based cancer therapy has been to identify promising targets involved in cancer progression and has been applied in clinical trials.[23,24]

Based on our previous findings, we present a novel nanocarrier design that can be utilized for mucin-triggered disassembly and consequent intestinal epithelial cellular entry of gapmers (Fig. 1). In this work, we investigated chitosan/gapmer nanocarrier formation and integrity in the presence of porcine gastric mucins using a fluorescence activation-based reporter system. Advanced 3D cell-based gut models of mucus-producing HT-MTX mono-culture and co-culture with adenocarcinoma Caco-2 cells were then used to evaluate gapmer and chitosan/gapmer cancer cell uptake compared to standard chitosan/siRNA designs. Furthermore, *in vivo* gapmer uptake in the murine GI tract was investigated by histological analysis using *in situ* gut loops.

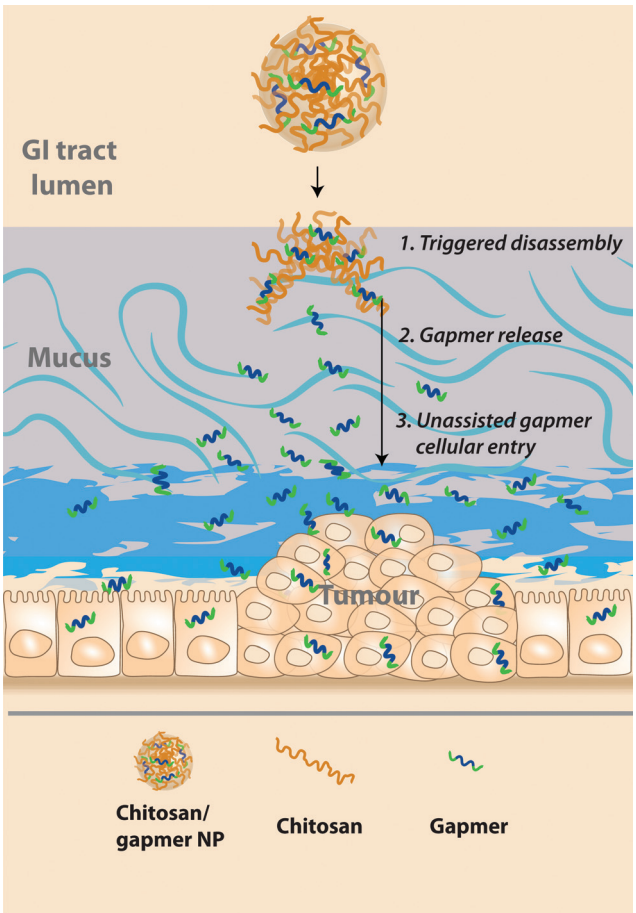

Fig. 1 Schematic representation of the nanocarrier design and triggered entry of gapmers into mucosal tissue. After oral administration the chitosan/gapmer nanocarriers encounter mucus (blue) and epithelial (beige) barriers. Mucus-triggered disassembly of chitosan/gapmer nanocarriers occurs enabling unassisted uptake of gapmers by epithelial cells and tumour cells in the gastrointestinal tract.

Materials and methods

Cell cultures

Human colon adenocarcinoma Caco-2 (passage 10–30) and mucus-secreting HT-MTX (passage 5–20) cells (both obtained from ATCC, Manassas, VA) were grown in Dulbecco modified Eagle's minimal essential medium with 4.5 g per L glucose (Gibco, Life technologies). Media was supplemented with 10% (v/v) fetal bovine serum (FBS) (Gibco, Life technologies), 1% (v/v) nonessential amino acids, 1% (v/v) L-glutamine and 1% (v/v) (all form Lonza, Verviers, Belgium). Cells were cultured at 37 °C under 5% CO_2 in a water saturated atmosphere.

HT-MTX cells alone, or in co-culture with Caco-2 cells at 1/10 ratio, were grown in Transwell™ polycarbonate inserts with 0.4 μm pore size (Corning-Costar, NY) pre-coated with Matrigel™ basement membrane matrix (Becton Dickinson, Bedford, MA) as described in Martirosyan *et al.*[25] The mucus production in the mono- and co-cultures was assessed by the Alcian Blue staining (10 mg ml^{-1}). Briefly, Alcian Blue (Sigma, Steinheim, Germany) dissolved in 3% acetic acid was added to the monolayer and incubated for 30 min at room temperature. The excessive Alcian Blue was removed by washing three times with PBS and cells on the membrane inserts were visualized by light microscopy.

Purification of porcine gastric mucins (PGM)

PGM (Type III, Sigma Aldrich) was purified as described in Thomsen *et al.*[19] Briefly, mucins were diluted in deionized water and stirred for 48 h at 4 °C. Afterwards a dialysis with a molecular weight cut-off of 1000 Da was performed (Spectra Pore Dialysis Membrane) against deionized water for 72 h at 4 °C. The purified mucins were then lyophilized and reconstituted in simulated intestinal fluid (SIF) prepared according to the International Pharmacopoeia[26] to reach a final mucin concentration of up to 2% w/v.

Production and characterization of nanocarriers

In this study a conventional 21-mer siRNA and 13-mer phosphorothioated gapmers were used, both labeled with 5-carboxyfluorescein (5-FAM). Oligonucleotides sequences were: siRNA (GenePharma, Shanghai, China) 5′-UUC UCC GAA CGU GUC ACG UTT (sense) and 5′-ACG UGA CAC GUU CGG AGA ATT (antisense); gapmer (RiboTask, Odense, Denmark) 5′-lAlCdCdCdAdTdCdGdGdCdTlGlG (l – locked nucleic acid, d – deoxyribonucleotide).

Nanocarriers composed of chitosan (36.8 kDa, 87.9% deacetylated, Synolyne Pharma, BE) and oligonucleotides were pre-

pared by a bulk formulation method by electrostatic self-assembly of the component parts.[27] Chitosan was first dissolved in sodium acetate buffer (300 mM, pH 5.5) and an appropriate amount of gapmers or siRNA were then added by slow continual motion, whilst stirring, to obtain the desired ionic balance of the complexes, measured as a number of amino groups of chitosan (N) per oligonucleotide phosphate (P) – N : P ratio (10, 60 and 120). The mixture was left to stir for an hour at room temperature.

Nanoparticle tracking analysis (NTA) (Nanosight LM10 system, Malvern Instruments, Southborough, MA) was used to measure the size, and the Zetasizer NanoZS-90 based on Laser Doppler Micro-Electrophoresis (Malvern Instruments, Southborough, MA) was used to measure the zeta potential of the chitosan/gapmer and chitosan/siRNA nanocarriers at N : P 60 in acetate buffer. Oligonucleotides encapsulation was evaluated indirectly by measuring the nanoparticles fluorescence quenching at λ_{ex} 485 nm and λ_{em} 520 nm (SpectraMax M3, Molecular Devices).

Mucin-triggered oligonucleotides release from nanocarriers

The release and the dissociation kinetics of gapmers or siRNAs from the nanocarriers were studied by fluorescence spectroscopy. The changes in the characteristic peak of 5-FAM-labeled oligonucleotides (λ_{em} = 520 nm) upon complexation with chitosan and emission spectra of nanoparticles were analyzed with FlouoroMax-3 (Horiba) in cuvettes with a 1 cm path length. To study the release kinetics of oligonucleotides from nanoparticles samples were analyzed in black 96-well plates in a BMG FLUOstar OPTIMA Microplate Reader set to excitation at 485 nm and emission at 520 nm. The release rate was calculated *via* the formula:

$$R = (F_{\text{disassembly}} - F_{\text{bound}})/(F_{\text{free}} - F_{\text{bound}})$$

where R is the amount of free FAM-oligonucleotide, $F_{\text{disassembly}}$ is the fluorescence emission from the nanoparticle solution at a given time point, F_{free} – fluorescence emission from naked FAM-oligo, F_{bound} – fluorescence emission from discrete chitosan/FAM-oligonucleotide nanoparticles.

In vitro cellular uptake studies

In vitro uptake of oligonucleotides was studied in mucus producing HT-MTX mono-cultures and HT-MTX/Caco-2 co-cultures. After 48 h (poorly differentiated) or 21 days (well-differentiated) post-seeding cells were washed twice with PBS and subsequently gapmer, siRNA or their polyplexes were applied and incubated for 24 h at 37 °C and 5% CO_2 to reach a final oligonucleotide concentration of 100 nM. The cells were then washed twice with PBS, harvested by tripsinization and fixed with 2% paraformaldehyde solution containing 1% FBS for flow cytometric analysis (Gallios, Beckman Coulter), or fixed with 4% paraformaldehyde for 15 min, permeabilized and stained with Hoechst 33342 (Life technologies) for confocal microscopic analysis (LSM700, Zeiss).

Intestinal uptake studies using *in situ* gut loops

For the *in vivo* experiments female 8–10 week-old C57BL/6J mice (N = 2) were used (Janvier Labs). All animal experiments were performed with the approval from the Danish Experimental Animal Inspectorate and according to the Danish national and institutional regulations. The animals were anaesthetized with a mixture of 2–4% isoflurane in air, and an incision was made to access the abdominal cavity. Intestinal gut loops were then prepared by ligation either side of a selected region of the proximal and distal small intestine ~3.5 cm in length using surgical suture. 300–500 μl of either naked oligonucleotides (gapmers or siRNA) or in formulation with chitosan were then injected into the loops. After 30 min incubation, the animals were euthanized by cervical dislocation and the intestinal tissue was removed, flushed thoroughly with PBS and fixed with 4% paraformaldehyde in PBS for 4–5 hours. Samples were then left overnight in a 0.4% paraformaldehyde/PBS solution at 4 °C. Tissue was then embedded in paraffin as previously described in Moeller *et al.*[28] 4 μm sections were cut using a rotary microtome (Leica Microsystems, Ballerup, Denmark) followed by paraffin removal using xylene and rehydration in graded alcohols. Sections were then stained with TO-PRO3 (Invitrogen) to visualize the nuclei, rinsed several times in PBS and mounted using antifade mounting media (Dako, Glostrup, Denmark) before analysis by confocal microscopy (LSM700, Zeiss).

Statistical analysis

For statistical analysis JMP (version 11 form SAS) was used. Data is presented as means ± SD. Comparison of groups was performed by Student's t-test, while comparison of more than two groups was performed using ANOVA. Differences were considered significant at $p < 0.05$.

Results

Preparation and physicochemical characterization of nanoparticles

The analysis of fluorescence emission spectra of FAM-labelled nucleic acids revealed a fluorescence intensity decrease or quenching after particle formation with chitosan for both gapmer ~90% and siRNA ~65% compared to naked oligonucleotide fluorescence (Fig. 2).

Chitosan/gapmer nanocarriers formed at N : P 60 were found to be ~150 nm in diameter by NTA (Table 1). Zeta potential measurements showed an overall positive charge of the nanocarriers with both gapmers and siRNA (Table 1), however, higher values were obtained for the chitosan/siRNA particles than the chitosan/gapmer nanocarriers. This may indicate greater electrostatic interaction and more incorporation of excess polycation into the gapmer nanocarriers that may facilitate greater stability.

Whilst the fluorescence of 5-FAM was quenched upon chitosan complexation, complex dissociation and release of oligonucleotides restored the dye fluorescent signal and, therefore,

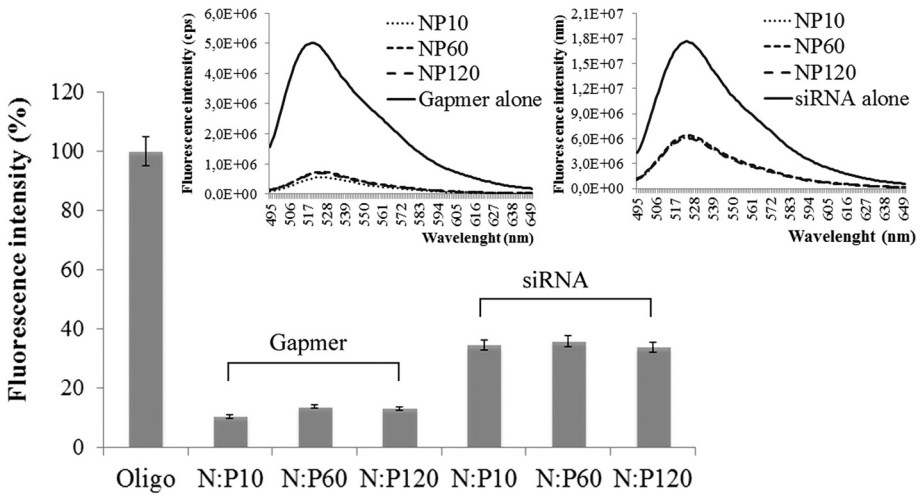

Fig. 2 Fluorescence quenching of FAM-labeled gapmer and siRNA upon complexation with chitosan at different N : P ratios (10, 60 and 120). The bar chart represents the fluorescence intensities of nanoparticles normalized to that of the free oligonucleotides. Emission spectra are given above.

Table 1 Size and zeta potential measurements of gapmer and siRNA complexes with chitosan

Nanocarrier	Size (nm)	ζ Potential (mV)
Chitosan/gapmer N : P 60	162.2 ± 7.8	7.04 ± 1.08
Chitosan/siRNA N : P 60	190.1 ± 10.8	13.74 ± 1.23

Representation of average of three determinations, (±) denote SD.

was used as a measure of particle integrity. Release of both gapmer (Fig. 3B) and siRNA (Fig. 3C) from the nanocarriers was shown following incubation with porcine gastric mucins (PGM), where the level of release was dependent on N : P ratio, contact time and mucin concentration. Within the observed time period of 75 min, a maximal gapmer release of ~25% and siRNA release of ~56% was observed from nanocarriers formed at N : P 10. Lower release rates were observed at higher N : P ratios (Fig. 3B), *e.g.* a gapmer release of ~20% and ~13% was revealed from chitosan/gapmer nanocarriers at N : P 10 and 120, respectively after 1 h incubation with PGM.

An increased release level was observed at higher PGM concentrations, which was more obvious in the case of siRNA (Fig. 3A). A release of gapmers ~6% and ~8.5% from nanocarriers at N : P 10 was observed following incubation with 0.5% and 2% PGM, respectively 30 min post-incubation. In the same conditions an siRNA release of ~16% (at 0.5% PGM) and ~44% (at 2% PGM) was observed from the chitosan/siRNA nanocarriers. This data suggests higher stability of nanocarriers containing gapmers, and that the release rates in the presence of mucins can be tuned by the composition of the nanocarrier which may have implications for therapeutic applications.

Biological studies

Poorly- and well-differentiated mono- and co-culture systems of mucus-secreting epithelial HT-MTX and the carcinoma epithelial cell line Caco-2 were used to study the influence of mucus on the *in vitro* uptake of oligonucleotides. Validation of the mucus production in the cells was performed by Alcian Blue staining that binds and stains blue the acidic mucopolysaccharides found in the goblet cells of the intestine.[29] More mucin staining was apparent in mucus-producing HT-MTX mono-cultures, compared with the HT-MTX/Caco-2 cells co-culture (Fig. 4A).

Cell viability in differentiating HT-MTX mono-cultures and HT-MTX/Caco-2 co-cultures was maintained after the addition of naked gapmer, siRNA and respective chitosan complexes measured using a LDH assay (ESI Fig. 1†). Cellular uptake of gapmer or siRNA, either naked or in combination with chitosan, was evaluated by confocal microscopy (Fig. 4) and flow cytometry (Fig. 5). Confocal microscopy analysis revealed, in contrast to naked siRNA, that gapmers were capable of entry into differentiating intestinal epithelial cells unassisted. The nanocarrier formulations adhered to the cell surface and formed aggregates with the mucus-producing mono-cultures, whilst in the co-cultures only small aggregates were observed (Fig. 4C and E). Greater aggregation of nanocarriers was seen for both gapmer and siRNA formulations at the epithelial–mucus interface of the mucus-producing HT-MTX cells that supports chitosan mucoadhesion.

No uptake was observed, however, in the fully differentiated intestinal epithelial cells with both types of nucleic acids in naked or nanoparticle form over the time period investigated by confocal microscopy (data not shown).

A significant cellular fluorescence increase was observed by flow cytometric analysis in both mono- and co-cultures incubated with gapmer, chitosan/gapmer and chitosan/siRNA nanocarriers at N : P 60, but not naked siRNA (Fig. 5). This data in combination with the confocal images provides direct evidence that gapmers can enter poorly-differentiated intestinal epithelial cells unassisted (Fig. 4 and 5). The incorporation of gapmers into nanocarriers at N : P 60 did not improve sig-

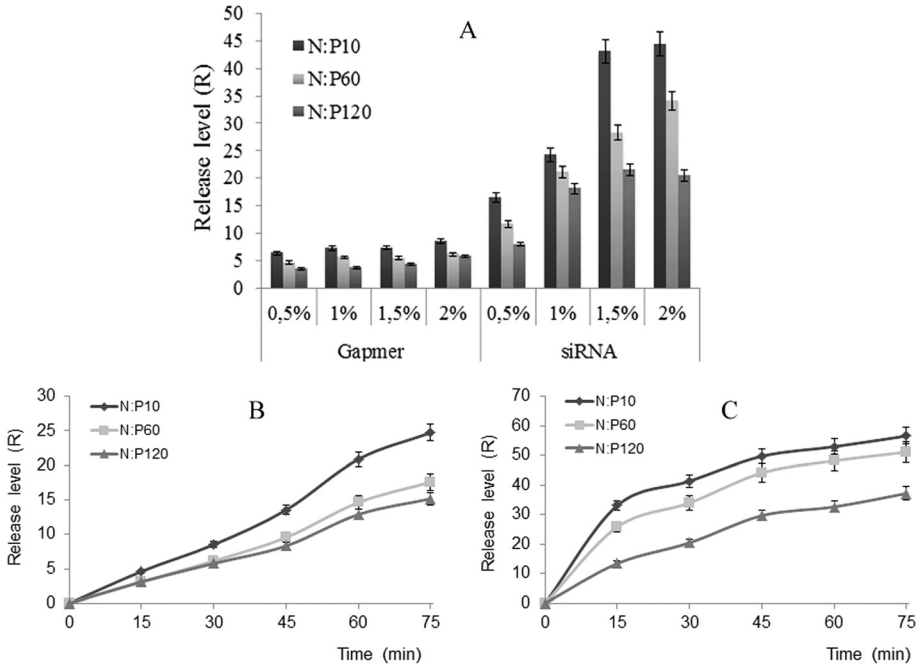

Fig. 3 The release levels (*R*) of gapmer and siRNA from nanocarriers at different N : P ratios (10, 60 and 120) in the presence of PGM at 2% after incubation of 30 min (A). Kinetics of the gapmer (B) and siRNA (C) release from nanocarriers depending on the incubation time and PGM concentration (0.5%–2%). The fluorescence intensities were normalized to the initial fluorescence intensities observed at 0 time point.

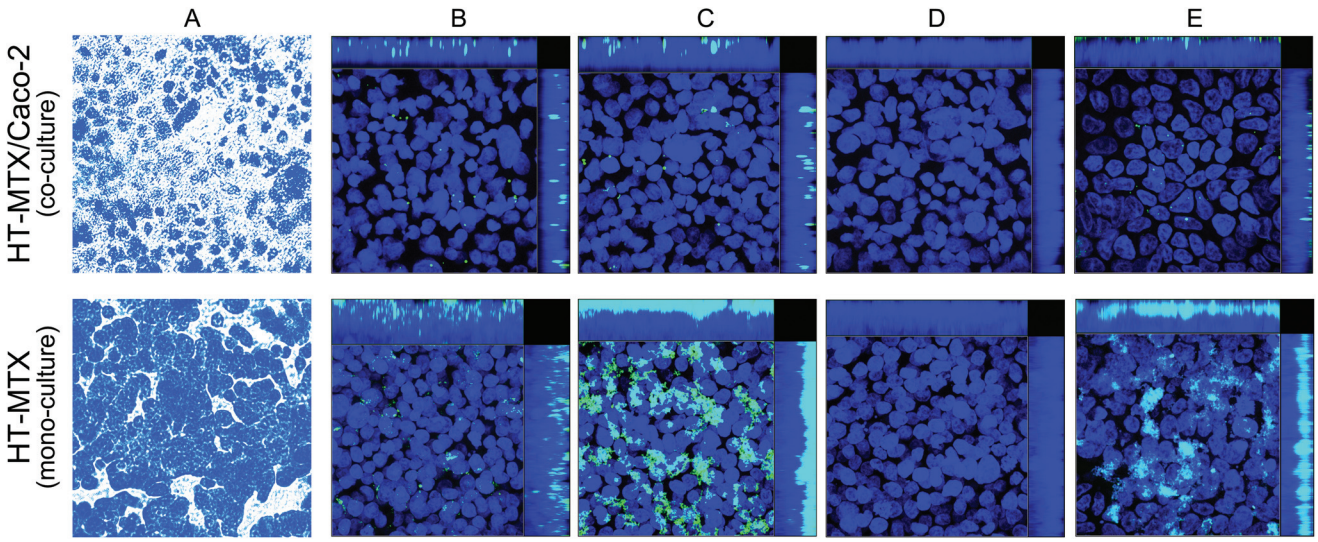

Fig. 4 Confocal laser scanning microscopy images of differentiating mono- and co-cultures exposed to gapmer (B), chitosan/gapmer (C), siRNA (D) and chitosan/siRNA (E) for 24 h at 37 °C. The oligonucleotides concentration was 100 nM, the nanocarriers were at N : P 60. The oligonucleotides were labeled with 5-FAM (green) and cell nuclei with Hoechst 33342 (blue). Mucus production in mono- and co-cultures was visualized by Alcian Blue staining (A).

nificantly the gapmer uptake (Fig. 5A). Similar uptake levels were observed for both mono- and co-culture systems. No uptake was shown with gapmer and siRNA either naked or within nanocarriers in the well-differentiated intestinal epithelial cells (Fig. 5B). Gapmers, however, were capable of entry into in the mucus-producing well-differentiated mono-culture system (Fig. 5B).

In vivo uptake of FAM-labelled oligonucleotides either naked or in combination with chitosan was investigated using *in situ* gut loops in adult mice ($N = 2$). The samples were

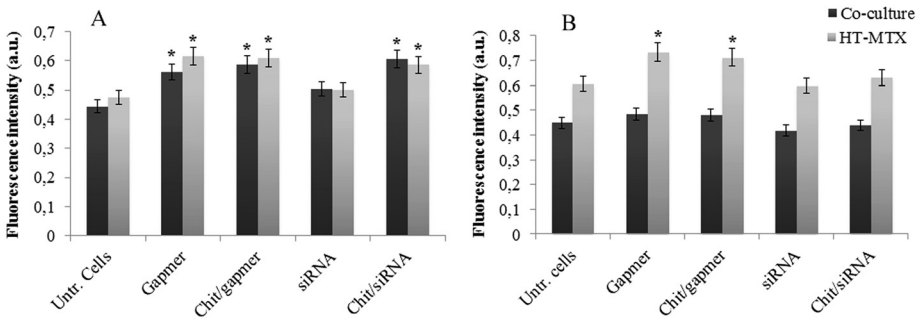

Fig. 5 Gapmer and siRNA uptake (100 nM, 24 h incubation time) by poorly-differentiated (A) and well-differentiated (B) mono- (HT-MTX) and co-cultures (HT-MTX/Caco-2) analysed by flow cytometry. 5000 events were registered for each analysis with at least 10^6 cells per ml. *Samples significantly different from the control (N = 2, n = 3, $p < 0.05$).

injected into the intestinal loops at the distal small intestine and allowed direct contact with the mucus/epithelial surface. After 30 minutes the tissue was harvested, paraffin sections of intestinal tissue were prepared and analysed by confocal microscopy (Fig. 6). The background autofluorescence of cells was eliminated enabling accurate and precise measurements of the 5-FAM signal.

Histological analysis revealed intracellular fluorescence of naked gapmers, but not naked siRNA (Fig. 6b and e, respectively). The gapmers were present within all epithelial cells with greater accumulation in the crypts region (Fig. 6b). Incorporation of gapmers in nanocarriers led to fluorescence intensity decrease compared to naked gapmers in the histological sections. Greater tissue fluorescence was observed for chitosan/gapmer nanocarrier samples at N : P 60 compared to N : P 120 (Fig. 6c and d, respectively). The chitosan/siRNA nanocarrier seemed to show accumulation around the intestinal villi with no observed fluorescence in the crypts (Fig. 6f).

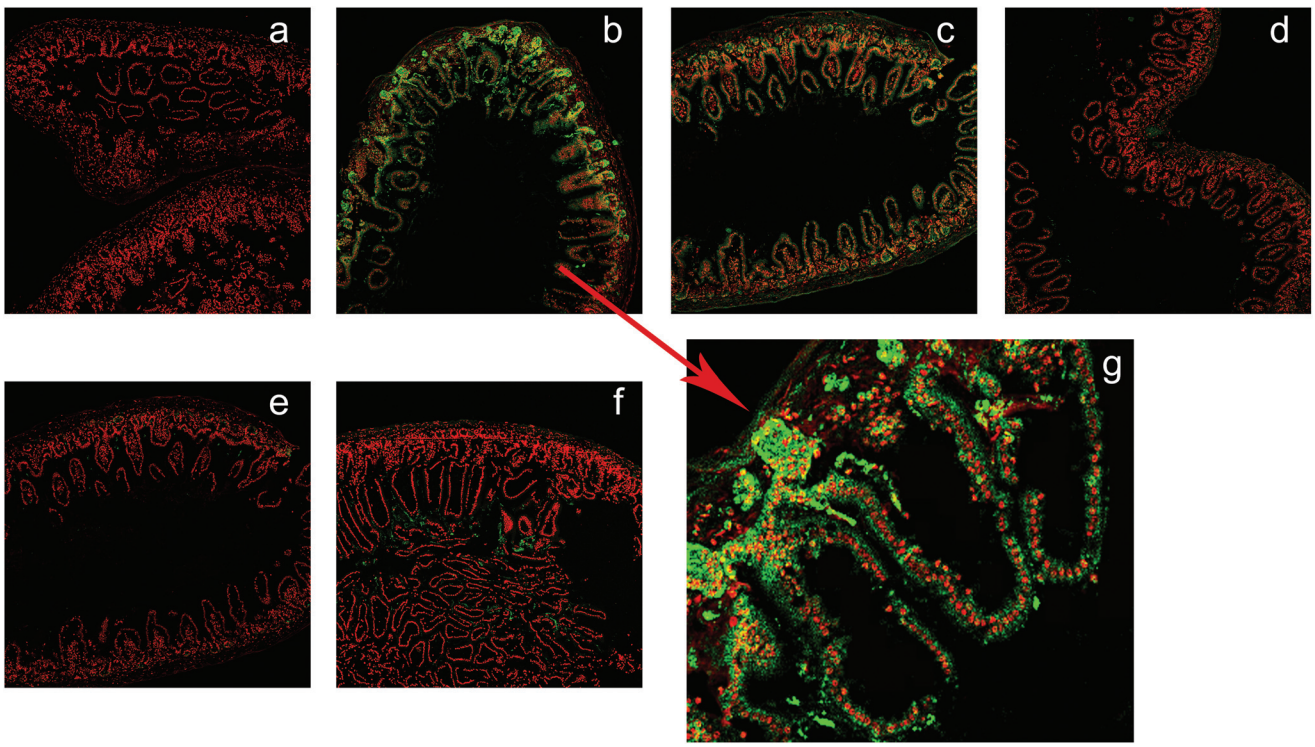

Fig. 6 Representative images of 4 μm paraffin sections of gut loops exposed to gapmers (b), chitosan/gapmer at N : P 60 (c), chitosan/gapmer at N : P 120 (d), siRNA (e) and chitosan/siRNA at N : P 60 (f) in the intestine after 30 min exposure in the *in situ* gut loops performed in 8–10 week-old female C57BL/6J mice (N = 2). The acetate buffer was injected as a control (a). Both the gapmer and siRNA were applied at a concentration of 4 μM with 300–500 μl injection into each gut loop (~3.5 cm). 5-FAM-labeled gapmers (green) could be detected in and/or around the intestinal epithelial cells. Zoomed image is provided for the naked gapmer uptake (g). Nuclei were labeled with TO-PRO-3 (red).

Discussion

The potential oral applications of RNAi-based therapeutics for treatment of intestinal tumours rely on the development of enabling delivery solutions able to overcome the mucin barrier and reach the cancer cell. Recent work from our lab suggests a possibility to exploit mucosal barrier interaction to trigger the site-specific release of the therapeutic from a mucoadhesive nanoparticle.[19] The inability of siRNA to enter cells after release, prompted us to redesign a mucoadhesive particle to contain a nucleic acid therapeutic capable of unassisted cellular entry. This work describes a simple approach to trigger the uptake of antisense gapmers at mucosal sites following protection afforded by the chitosan during gastric transit.

We first investigated formation of chitosan nanocarriers using gapmers of 13 nucleotide length. NTA revealed formation of particles ~150 nm in size similar to siRNA of ~190 nm that suggested minimal differences between single and double stranded oligonucleotides on the formation process (Table 1). Interestingly, higher positive surface charge was apparent in the siRNA particle that could reflect the presence of an excess chitosan not involved in electrostatic interaction that could reduce stability.

The close proximity of two identical FAM-labeled molecules and consequent interaction of fluorophores has been shown to induce fluorescence quenching involving a combination of trap-site formation and resonance energy transfer between the fluorophores due to a small stokes shift.[30,31] This feature has been used previously by our group to monitor nanocarrier formation using FAM-labelled siRNA with chitosan.[19] A fluorescence quenching of 5-FAM-labeled gapmers occurred upon interaction with chitosan (Fig. 2) suggesting recruitment into a discrete particle. Comparative analysis of gapmers and siRNA complexation with chitosan revealed more efficient encapsulation of gapmers with a higher level of fluorescence quenching, compared to that of siRNA (Fig. 2) that may support increased stability for the gapmer formulation.

Nanocarrier disassembly and oligonucleotide release was triggered in the presence of PGMs, reflected by the restored fluorescence intensity of 5-FAM (Fig. 3). Chitosan has been shown previously to interact with the mucins, the predominant component of mucus, based on electrostatic interaction of its amino groups with the negatively charged binding sites of the mucin fibers such as sialic groups.[13,32] The kinetics of nanocarrier disassembly differed for the gapmer and siRNA-based systems. A steady release of gapmers was shown over the observed time period of 75 min, whilst a more rapid release for the first 30 min was shown for the siRNA (Fig. 3). The release of both gapmer and siRNA from nanocarriers was dependent on N : P ratio, interaction time with PGMs, as well as on PGMs concentration (Fig. 3). Less release of oligonucleotides was observed at higher N : P ratios that possibly reflects increased stability shown previously for nanocarriers at high N : P.[16] Furthermore, the PGM concentration increase resulted in higher disassembly level for both types of nanocarriers. Previous work indicated decreased stability of chitosan/siRNA nanocarriers at the higher N : P 60 upon contact with PGM,[19] this could possibly reflect the presence of more excess amounts of chitosan available for mucin interaction supported by the larger nanocarrier size compared to that shown in the present work. The ability to tune oligonucleotide release using particles at different N : P opens new possibilities to tailor the therapeutic profile at mucosal sites. Less release was observed for the nanocarriers containing gapmers compared to siRNA that can be attributed to greater stability which may have advantages in protection against the harsh chemical and enzymatic conditions found within the GI tract.

The basis of this work is an ability of unassisted epithelial entry of released oligonucleotides as a consequence of nanocarrier contact with mucus. The application of mucus secreting mono- and co-culture epithelial cell-based models allowed us to investigate this. Caco-2 and HT-MTX represent the two most abundant cell populations in the intestinal epithelium – absorptive cells and mucus-producing goblet cells and, hence, their co-cultures provide a drug absorption model incorporating the mucus barrier.[33] It was shown that gapmers, but not siRNA exhibited unassisted uptake in poorly-differentiated intestinal epithelial cells, but neither were capable of uptake in well-differentiated ones (Fig. 4 and 5). Observed results are in agreement with existing evidence that short antisense oligonucleotides can enter the cells unassisted, demonstrated in different cell types.[20,21] After entering the cells, LNA/DNA/LNA gapmers were reported to induce RNase H activation and hence, cleavage of the target mRNA.[22,34] Gymnosis has been demonstrated in different cell-based systems,[20,21] while no uptake was shown in the case of confluent cells.[20] This tendency was also seen in our work, since no gapmer uptake was revealed in well-differentiated co-cultures that could be potentially improved by increase in gapmer concentration and/or incubation time.

Inclusion within chitosan nanocarriers did not influence the cell uptake for gapmers in poorly-differentiated cells, while significantly improved the uptake of siRNA (Fig. 5A). The latter was also confirmed by previous studies, suggesting that complexation with chitosan facilitates the siRNA uptake.[16,18] Nanocarriers were shown to be attached to the surface of the cell monolayer in the mucus-producing cell mono-cultures (Fig. 4C and E) that supports interaction with mucins. In contrast, no nanocarrier aggregation at the mucin/liquid interface was evident in the co-culture systems, where the mucus production was shown by Alcian Blue to be less. These findings suggest that mucoadhesive properties of chitosan are favouring the nanocarrier trapping in the mucus layer and likely confirm the existing data that mucoadhesive nanoparticles can aggregate on the surface of the mucus barrier.[35]

An *in vivo* investigation into the biological performance of gapmer formulations was conducted using murine intestinal loops. Upon exposure to naked gapmers a green fluorescence was observed within the intestinal tissue (Fig. 6b), suggesting that the 5-FAM-labeled gapmers likely enter the gut cells unassisted in contrast to the siRNA (Fig. 6e). It is worth noting that no green signal was observed in the case of exposure to the

5-FAM dye alone neither *in vitro*, nor *in vivo* (data not shown). The uptake of gapmers within nanocarriers was dependent on the N : P ratio, with less uptake at higher N : P (Fig. 6d) that may reflect increased stability in the presence of mucus (Fig. 2 and 3). A similar aggregation of chitosan/gapmer and chitosan/siRNA nanoparticles was observed in the *in vivo* tissue (Fig. 6) and mucus-producing cell line (Fig. 4). A preferential accumulation of gapmers in the intestinal crypts was seen (Fig. 6b and g) that could be likely explained by the presence of dividing stem cells in crypts, a region responsible for the cell renovation of the GI epithelium.[36] Various mucoadhesive nanoparticle delivery systems have been studied to achieve efficient mucosal delivery of drugs. Particularly, cationic polymethacrylate-based nano-delivery system was applied for rectal administration of clodronate-loaded nanoparticles,[37] which was successful in alleviating the inflammatory response in murine colitis models. Interestingly, interaction with mucin obstructed the transport of cationic nanoparticles through the mucus layer, increasing the risk of premature drug release by an ion exchange mechanism. In another study, Lautenschlager *et al.*[38] assessed the *ex vivo* targeting potential of chitosan-functionalised poly(lactic-*co*-glycolic acid) nanoparticles to human GI mucosa and showed that nanoparticles were able to adhere onto the tissue surface, however, with minimal particle translocation and deposition. Alternative approaches, such as oxidative stress-responsive thioketal nanoparticles for oral delivery of siRNA to the sites of intestinal inflammation were developed that degrades and releases siRNA selectively in response to reactive oxygen species.[39] However, the elaborate designs of these nanoparticles used would seemingly restrict early clinical translation.

RNAi-based therapeutics provides a tool to target and control the tumor progression *via* silencing the expression of cancer-relevant proteins with high selectivity. The current knowledge on the use of RNAi techniques in the cancer treatment and potential targets are summarised in recent reviews.[4,40] Antisense oligonucleotides represent a highly specific tool with already numerous promising targets for cancer therapy[23,24] with many more to be revealed with cancer genomic, transcriptomic and proteomic data.

The fact that the gapmer release from the nanocarrier was influenced by the mucins concentration (Fig. 3) may be exploited for increased triggered-release at the sites of adenocarcinomas, *e.g.* pancreatic, lung, breast, ovarian and colorectal with upregulated mucin levels.[41,42] Whilst, mucin has been utilised in this work for triggered disassembly of the nanocarriers, mucins may also offer a potential silencing target due to possible implications in cancer development and progression, and protection against the host immune response.[41] Recently, mucins have been used as targets for immunotherapy, gene therapy and other novel therapeutic strategies for cancer treatment.[43,44] For instance, studies that evaluated levels of MUC1 expression on clinical samples indicate that overexpression of MUC1 was associated with invasive and metastatic tumours of the colon, pancreas, gall bladder and oral epithelium.[45] Targeted inactivation of murine Muc1 significantly reduced the growth rate of oncogene-induced mammary tumours and mildly affected the propensity for these tumours to metastasize.[46]

The application of our system is dependent on the mucosal silencing activity of the released oligonucleotides that is presently being investigated in our lab. Furthermore, further optimization to gain efficient balance between protection, mucoadhesion and the triggered-release rate and amount of gapmers is needed. Improved design of the mucin-triggered drug delivery system together with a greater understanding of the molecular and genetic abnormalities driving transformation may allow the design of oligonucleotide-based personalized cancer medicines.

Conclusions

This work presents a novel chitosan nanocarrier design for mucin-triggered release of gapmers for unassisted entry into intestinal epithelial cells. N : P ratio, incubation time and mucin concentration influenced particle disassembly and release rate in porcine gastric mucins. Mucin-secreting intestinal epithelial mono- and co-culture models and *in situ* gut-loops showed chitosan-mediated adhesion to the mucus layer, and unassisted naked gapmer uptake in contrast to naked siRNA. The findings present a mucosal design-based system for local delivery of oligonucleotides that may improve the effectiveness of gene silencing therapeutics at mucosal sites to treat mucus-associated diseases, such as cancer.

Acknowledgements

The authors thank Prof. Jesper Wengel (BioNEC – A VKR Center of Excellence FKF, University of Southern Denmark) for providing the FAM-labeled gapmers, Xenia Lefebvre (Synolyne Pharma, Herstal, Belgium) for providing the chitosan and Inger Merete Paulsen for excellent technical assistance with the *in vivo* work. This work was supported by the NanoBar grant (Project number 904280) from the Danish Strategic Research Council and by the EU-FP7 HEALTH-2010-259842 (ANTIFLU) grant. The authors declared no conflict of interest.

References

1 Cancer Classification of the National Cancer Institute, http://training.seer.cancer.gov/disease/categories/classification.html accessed on 15 October 2015.
2 M. Malvezzi, P. Bertuccio, T. Rosso, M. Rota, F. Levi, C. La Vecchia and E. Negri, *Ann. Oncol.*, 2015, 1–8.
3 E. Miele, G. P. Spinelli, E. Miele, E. Di Fabrizio, E. Ferretti, S. Tomao and A. Gulino, *Int. J. Nanomed.*, 2012, **7**, 3637–3657.
4 B. Ballarín-González, M. F. Ebbesen and K. A. Howard, *Cancer Lett.*, 2014, **352**, 66–80.

5 S. Y. Wu, G. Lopez-Berestein, G. A. Calin and A. K. Sood, *Sci. Transl. Med.*, 2014, **6**, 240ps7.
6 K. A. Howard and J. Kjems, *Expert Opin. Biol. Ther.*, 2007, **7**, 1811–1822.
7 K. A. Howard, *Adv. Drug Delivery Rev.*, 2009, **61**, 710–720.
8 M. T. J. Olsesen, B. Ballarín-González and K. A. Howard, *Drug Delivery Transl. Res.*, 2014, **4**(1), 4–18.
9 S. K. Linden, P. Sutton, N. G. Karlsson, V. Korolik and M. A. McGuckin, *Mucosal Immunol.*, 2008, **1**, 183–197.
10 S. K. Lai, Y.-Y. Wang, D. Wirtz and J. Hanes, *Adv. Drug Delivery Rev.*, 2009, **61**, 86–100.
11 R. Bansil, J. P. Celli, J. M. Hardcastle and B. S. Turner, *Front. Immunol.*, 2013, 310.
12 M. S. Draz, B. A. Fang, P. Zhang, Z. Hu, S. Gu, K. C. Weng, J. W. Gray and F. F. Chen, *Theranostics*, 2014, **4**, 872–892.
13 L. Illum, I. Jabbal-Gill, M. Hinchcliffe, A. N. Fisher and S. S. Davis, *Adv. Drug Delivery Rev.*, 2001, **51**, 81–96.
14 A. Martirosyan, M. J. Olesen and K. A. Howard, *Adv. Genet.*, 2014, **88**, 325–352.
15 K. A. Howard, U. L. Rahbek, X. Liu, C. K. Damgaard, S. Z. Glud, M.Ø. Andersen, M. B. Hovgaard, A. Schmitz, J. R. Nyengaard, F. Besenbacher and J. Kjems, *Mol. Ther.*, 2006, **14**, 476–484.
16 X. Liu, K. A. Howard, M. Dong, M.Ø. Andersen, U. L. Rahbek, M. G. Johnsen, O. C. Hansen, F. Besenbacher and J. Kjems, *Biomaterials*, 2007, **28**, 1280–1288.
17 E. J. B. Nielsen, J. M. Nielsen, D. Becker, A. Karlas, H. Prakash, S. Z. Glud, J. Merrison, F. Besenbacher, T. F. Meyer, J. Kjems and K. A. Howard, *Pharm. Res.*, 2010, **27**, 2520–2527.
18 B. Ballarín-González, F. Dagnaes-Hansen, R. A. Fenton, S. Gao, S. Hein, M. Dong, J. Kjems and K. A. Howard, *Mol. Ther. Nucleic Acids*, 2013, **2**, e76.
19 T. B. Thomsen, L. Li and K. A. Howard, *Nanoscale*, 2014, **6**, 12547–12554.
20 C. A. Stein, J. B. Hansen, J. Lai, S. Wu, A. Voskresenskiy, A. Hog, J. Worm, M. Hedtjarn, N. Souleimanian, P. Miller, H. S. Soifer, D. Castanotto, L. Benimetskaya, H. Orum and T. Koch, *Nucleic Acids Res.*, 2010, **38**, e3.
21 S. A. Moschos, M. Frick, B. Taylor, P. Turnpenny, H. Graves, K. G. Spink, *et al.*, *Mol. Ther.*, 2011, **19**, 2163–2168.
22 C. Wahlestedt, P. Salmi, L. Good, J. Kela, T. Johnsson, T. Hökfelt, *et al.*, *Proc. Natl. Acad. Sci. U. S. A.*, 2000, **97**, 5633–5638.
23 D. Castanotto and C. A. Stein, *Curr. Opin. Oncol.*, 2014, **26**, 584–589.
24 P. M. Moreno and A. P. Pêgo, *Front. Chem.*, 2014, **2**, 87.
25 A. Martirosyan, A. Bazes and Y.-J. Schneider, *Nanotoxicology*, 2014, **8**, 573–582.
26 The International Pharmacopoeia, 5th edition http://apps.who.int/phint/en/p/docf/ accessed on 15 September 2015.
27 M.Ø. Andersen, K. A. Howard and J. Kjems, *Methods Mol. Biol.*, 2009, **555**, 77–86.
28 H. B. Moeller, M. A. Knepper and R. A. Fenton, *Kidney Int.*, 2009, **75**, 295–303.
29 K. Matsuo, H. Ota, T. Akamatsu, A. Sugiyama and T. Katsuyama, *Gut*, 1997, **40**, 782–789.
30 K. Zhou, H. Liu, S. Zhang, X. Huang, Y. Wang, G. Huang, B. D. Sumer and J. Gao, *J. Am. Chem. Soc.*, 2012, **134**, 7803–7811.
31 L.-C. Ho, C.-M. Ou, C.-L. Li, S.-Y. Chen, H.-W. Li and H.-T. Chang, *J. Mater. Chem. B*, 2013, **1**, 2425–2432.
32 A. M. De Campos, A. Sanchez, R. Gref, P. Calvo and M. J. Alonso, *Eur. J. Pharm. Sci.*, 2003, **20**, 73–81.
33 G. J. Mahler, M. L. Shuler and R. P. Glahn, *J. Nutr. Biochem.*, 2009, **20**, 494–502.
34 J. Kurreck, E. Wyszko, C. Gillen and V. A. Erdmann, *Nucleic Acids Res.*, 2002, **30**, 1911–1918.
35 L. M. Ensign, C. Schneider, J. S. Suk, R. Cone and J. Hanes, *Adv. Mater.*, 2012, **24**, 3887–3894.
36 R. Okamoto and M. Watanabe, *J. Gastroenterol.*, 2004, **39**, 1–6.
37 W. Niebel, K. Walkenbach, A. Beduneau, Y. Pellequer and A. Lamprecht, *J. Controlled Release*, 2012, **160**, 659–665.
38 C. Lautenschlager, C. Schmidt, C. M. Lehr, D. Fischer and A. Stallmach, *Eur. J. Pharm. Biopharm.*, 2013, **85**, 578–586.
39 D. S. Wilson, G. Dalmasso, L. Wang, S. V. Sitaraman, D. Merlin and N. Murthy, *Nat. Mater.*, 2010, **9**, 923–928.
40 J. Prados, C. Melguizo, H. Roldan, P. J. Alvarez, R. Ortiz, J. L. Arias and A. Aranega, *BioDrugs*, 2013, **27**, 317–327.
41 D. W. Kufe, *Nat. Rev. Cancer*, 2009, **9**, 874–885.
42 H. Debunne and W. Ceelen, *Acta Chir. Belg.*, 2013, **113**, 385–390.
43 M. P. Torres, S. Chakraborty, J. Souchek and S. K. Batra, *Curr. Pharm. Des.*, 2012, **18**, 2472–2481.
44 D. Roulois, M. Grégoire and J.-F. Fonteneau, *BioMed Res. Int.*, 2013, 871936.
45 T. M. Horm and J. A. Schroeder, *Cell Adhes. Migr.*, 2013, **7**, 187–198.
46 A. P. Spicer, G. J. Rowse, T. K. Lidner and S. J. Gendler, *J. Biol. Chem.*, 1995, **270**, 30093–30101.